Article

Differential Studies of Argon Particle and Antiparticle Interactions: Present Status and Future Possibilities

Robert D. DuBois [1],* and Károly Tőkési [2]

1 Department of Physics, Missouri University of Science and Technology, Rolla, MO 65409, USA
2 Institute for Nuclear Research (ATOMKI), 4026 Debrecen, Hungary
* Correspondence: dubois@mst.edu

Abstract: Although the comparison of fully differential ionization data for particle and antiparticle impact provides the ultimate tests of theoretical models, only very low antiparticle beam intensities are available. Hence, few experiments of this type have been performed. Therefore, available experimentally obtained single and double differential cross-sections, which are much easier to obtain, are compared in order to demonstrate differences when only the projectile mass or charge (+1 or −1) is changed. Included in the comparison are cross-sections calculated for positron and electron impact using a three-particle classical trajectory Monte Carlo method. The calculated cross-sections provide independent information about the ejected electron and the scattered projectile contributions, plus information about the impact parameters, all as functions of the collision kinematics. From these comparisons, suggestions as to where future investigations are both feasible and useful are provided.

Keywords: particle; antiparticle; differential; ionization; argon; CTMC

1. Introduction

Following the discovery of the positron and antiproton, numerous experimental and theoretical projects have compared antiparticle–particle and particle–particle interaction data in order to investigate whether they are similar or fundamentally different. In the field of atomic physics, comparing particle and antiparticle impact data allows an investigation of interaction probabilities and kinematics where only the projectile mass or the sign of projectile charge has been changed. We remind the reader that changing the projectile mass influences the amount of momentum/energy transfer from the projectile to the target components while the sign of the projectile charge reverses the direction of the electric fields between the projectile and the target components. Based on the electron density picture of the atomic systems, an example of charge effects is that upon entering the electron cloud of the target, the projectile is subject to a net positive charge from the partially screened nucleus. Thus, the expectation is that an electron projectile will be slightly attracted and interact with a bound electron at smaller impact parameters than a positron projectile, which will be slightly repelled and interact at larger impact parameters. Assuming the same electron cloud densities for these impact parameters, this would result in a slightly larger cross-section for positron impact. These alterations, of course, will decrease with collision energy since the repulsive/attractive forces have less time to act. Also, at low collision energies, differing portions of the incoming flux act with other inelastic channels for positron and electron impact; hence, the above expectation does not apply.

Another expectation is that the direction of the electric field forces should cause an electron to scatter "away" from the target, whereas a positron should scatter "toward" the target, which means that for binary interactions, the ejected electron will move "toward" the nucleus for electron impact and "away" from the nucleus for positron impact. Thus, for electron impact, the ejected electron should undergo a stronger attraction towards the nuclear charge, resulting in a larger probability for ejected electrons to be observed in the

backward direction. With the availability of antiparticle data, it is possible to isolate and study these effects and more stringently test various theoretical models and assumptions.

Experimentally, the problem with providing data for such tests is that antiparticle beam intensities are orders of magnitude smaller that particle beam intensities, e.g., mA electron or proton beams are easily created, whereas typical positron and antiproton beam intensities are fA or smaller. Another problem is that to obtain these beam intensities for antiprotons has meant using a wide range of energies. Therefore, many comparisons of total cross-sections have been reported, whereas far fewer measurements of differential cross-sections resulting from antiparticle impact are available for comparison. The tables in [1] provide a listing of available measurements for positron impact. For antiproton impact, only total cross-section measurements are available ([2–5] and the references within). Ideally, a comparison of fully differential data is desired. But, because of the small cross-sections and low positron beam intensities that are currently available, only three laboratories have reported fully differential data ([6–8] and references therein). Comparisons on the fully differential level, e.g., for single ionization, cross-sections where the kinematics of the scattered projectile and ejected electron are fully defined, have generally shown that for heavier targets, such as argon and nitrogen, theory has difficulty in predicting the measured binary-recoil intensity ratios. See, for example, refs. [9,10]. As will be shown in the following figures, for positron impact, the cross-sections in the backward direction are considerably smaller than those in the forward direction, which is an additional experimental problem.

Therefore, the intent of the present paper is to show comparisons on the single and double differential level where, with respect to the fully differential level, the cross-sections are considerably larger. Using data that are currently available, combined with theoretical results obtained using the classical trajectory Monte Carlo (CTMC) method [11], we compare single and double differential cross-sections (SDCS and DDCS) and offer suggestions as to where future studies would be useful. We note that for some of the comparisons, data are available from several sources. In order to make the figures more readable, we have chosen data that we regard as "reliable and representative" for making our comparisons. Also, we have restricted our comparisons to interactions with an argon target because more differential data are available. We also only consider fast collisions, e.g., impact velocities (V_o) greater than 2 a.u., in order to avoid electron capture, positronium formation, and electron exchange processes. The overall message from these comparisons is to show where future studies on the single and double differential level might provide useful information for testing theoretical predictions regarding how simply changing the sign of the projectile charge or the projectile mass alters the inelastic cross-section.

2. Theory

The classical trajectory Monte Carlo (CTMC) method is a well-known method to describe atomic collisions and to calculate cross-sections. In the present work, the CTMC simulations were made using a three-body approximation where the many-electron argon atom is replaced by a one-electron atom. A summary of the detailed calculation procedure are available in [11]. Here, we give a shorter description of the used model. In our present model, the three particles (target nucleus, target electron, and projectile) are characterized by their masses and charges. A central model potential developed by Green [12] with Z (the nuclear charge), N (the total number of electrons in the target), and r (the distance between the nucleus and the target electron q), is written as

$$V(r) = q\frac{Z - (N-1)\left(1 - \Omega^{-1}(r)\right)}{r} = q\frac{Z(r)}{r}, \text{ where } \Omega(r) = \frac{\eta}{\zeta}\left(e^{r\zeta} - 1\right) + 1 \qquad (1)$$

The potential parameters ζ and η are such that they minimize the energy for a given atom or ion. Garvey et al. [13] obtained the following parameters for Ar: $\eta = 3.50$ and $\zeta = 0.957$ (in atomic units, a.u.). We note that this type of potential has further advantages,

because it has a correct asymptotic form for both the small Equation (2) values and the large Equation (3) values of r.

$$\lim_{r \to 0} Z(r) = Z \tag{2}$$

$$\lim_{r \to \infty} Z(r) = Z - (N - 1) \tag{3}$$

The Lagrange equation for the three particles can be written as:

$$L = L_K - L_V \tag{4}$$

where

$$L_K = \frac{1}{2} m_P \dot{\vec{r}}_P^2 + \frac{1}{2} m_e \dot{\vec{r}}_e^2 + \frac{1}{2} m_T \dot{\vec{r}}_T^2 \tag{5}$$

and

$$L_V = \frac{Z_P Z_e}{\left| \vec{r}_P - \vec{r}_e \right|} + \frac{Z_P Z_T \left(\left| \vec{r}_P - \vec{r}_T \right| \right)}{\left| \vec{r}_P - \vec{r}_T \right|} + \frac{Z_e Z_T \left(\left| \vec{r}_e - \vec{r}_T \right| \right)}{\left| \vec{r}_e - \vec{r}_T \right|} \tag{6}$$

$\vec{r}$, Z, and m are the position vector, the charge, and the mass of the noted particle (i.e., P: projectile; T: target core; e: target electron, respectively). The equations of motion can be calculated as:

$$\frac{d}{dt} \frac{\partial L}{\partial \dot{q}_i} = \frac{\partial L}{\partial q_i}, \qquad (i = P, e, T). \tag{7}$$

For a large number of incoming projectile trajectories, the classical equations of motion obtained by Equation (7) of the system were integrated with respect to time using the standard Runge–Kutta method for a given set of initial conditions. The initial parameters for the projectile ion, defined with respect to the center-of-mass of the target system, were position R_0 and impact parameter b, which was randomly selected. The initial momentum was determined using the impact velocity v_P, and the initial direction was chosen in the direction of the z axis. The target electron was initially confined to the nucleus and was subjected to a non-colombic potential described by Equation (1). See Reinhold and Falcón [14] for a comprehensive explanation of the methodology for determining the initial parameters of this active electron.

After solving the equations of motion for a large number of trajectories, the total, the energy and angular single differential, and the double differential cross-sections were obtained using the following expressions:

$$\sigma = \frac{2\pi b_{max}}{N_{tot}} \sum_{i=1}^{N_t} b_i, \tag{8}$$

$$\frac{d\sigma}{dE} = \frac{2\pi b_{max}}{N_{tot} \Delta E} \sum_{i=1}^{N_t} b_i \tag{9}$$

$$\frac{d\sigma}{d\Omega} = \frac{2\pi b_{max}}{N_{tot} \Delta \Omega} \sum_{i=1}^{N_t} b_i \tag{10}$$

$$\frac{d^2\sigma}{d\Omega dE} = \frac{2\pi b_{max}}{N_{tot} \Delta \Omega \Delta E} \sum_{i=1}^{N_t} b_i. \tag{11}$$

In Equations (8)–(11), N_{tot} is the total number of trajectories calculated for impact parameters less than b_{max}, N_t is the number of trajectories that satisfy the criteria for ionization, and b_i is the actual impact parameter for the trajectory corresponding to the ionization process under consideration in the energy interval ΔE and the emission angle interval $\Delta \Omega$ of the electron.

The statistical error for a given measurement has the form

$$\Delta\sigma = \sigma\left(\frac{N_{tot} - N_t}{N_{tot}N_t}\right).$$ (12)

Using this method, cross-sections for direct comparison with experimental data were calculated. We note that this classical method contains information about the pre- and post-collision effects from all particles. In addition, impact parameter information is available and various sorting techniques can be used in order to investigate correlations between the outgoing particle energies and directions.

3. Antiparticle and Particle Impact Comparisons

3.1. Total Cross-Sections (TCS)

Although the primary objective of this work is to compare single and double differential data, a brief discussion of how total cross-sections compare is in order. For this comparison, we used single ionization data reported by McCallion et al. for electron impact [15], data reported by Bluhme et al. [16] and Jacobsen et al. [17] for positron impact, data reported by DuBois and Manson for proton impact [18], and data reported by Paludan et al. for antiproton impact [3]. For impact velocities greater than 2 a.u., the cross-sections for all four projectiles agree within approximately 15%, which is roughly the uncertainties quoted for each. It should be noted that the published antiparticle data were placed on an absolute scale using various normalization methods with respect to electron impact data. The observed agreement implies that for single electron removal in fast collisions, any effect associated with projectile mass or sign of charge is quite small. For collision velocities of less than 2 a.u., the positron and proton cross-sections are in agreement with each other and are larger than the electron and antiproton cross-sections, in accordance with one of the expectations mentioned in the introduction. Interested readers are directed to the work of Montanari and Miraglia [19], where comparisons of multiple ionization for several atoms are made.

3.2. Single Differential Cross-Sections (SDCS)

For a more sensitive comparison, single differential cross-sections, either as a function of ejected electron and/or scattered projectile energy or as a function of electron emission and projectile scattering angle, are used. Such data for electron and proton impact are available, whereas only a few measurements have been taken for positron impact and, to our knowledge, no differential studies on antiproton impact have been attempted. For electron and proton impact, typical uncertainties are ~25%; for positron impact, the uncertainties are similar or larger and are also subject to the size of the cross-section, which introduces statistical uncertainties.

In Figure 1, we compare energy distributions reported for electron [20,21], proton [22], and positron impact [23]. In addition, we show the values we obtained using our CTMC model. Three impact energies are shown and Bethe scaling, e.g., dividing the cross-section by lnT/T, where T is the impact energy in atomic units, has been applied in order to present all the data in a single figure. Also, rather than a horizontal energy axis, the ejected electron or scattered projectile, velocity, v_{post}, with respect to the impact velocity, v_p, is used. Thus, for leptons, the maximum-scaled velocity is 1 and for protons, there is a rapid decrease in the cross-sections beginning at a scaled velocity of 2, i.e., the value obtained classically for elastic collisions between a massive projectile and a light target.
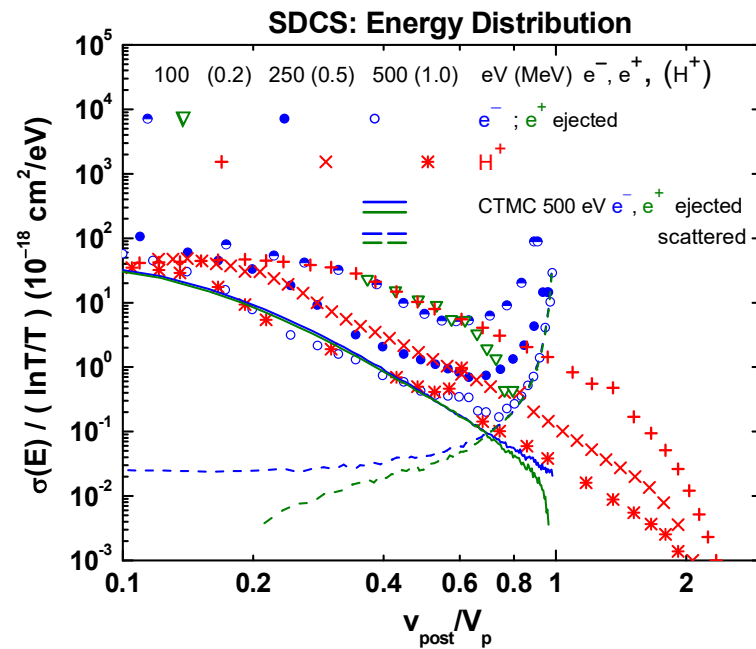
Figure 1. Bethe scaled single differential cross-section energy distributions for 100, 250, and 500 eV electron (blue circles) [20,21], positron (green triangles, scaled; see text) [23] (0.2 Crooks and Rudd, ref. [22]; 0.5 Gabler et al., ref. [22]; 1.0 MeV Toburen; ref. [22]), and proton impacts (red symbols); and our CTMC results for 500 eV electron and positron impacts (blue and green lines, respectively). Individual curves are shown for the ejected electrons and the scattered projectile CTMC results.

The measurement technique used to collect the electron and proton data did not discriminate against multiple or subshell ionization. However, multiple ionization contributes less than 10% [15,18] and 3s ionization should contribute less than 20% [24] to the cross-sections. Also, for electron impact the cross-section is the sum of the ejected electron and scattered projectile cross-sections. In contrast, the technique used for positron impact recorded only single ionization events on a relative scale. Here, we arbitrarily scaled the positron data. Our CTMC calculations are only for single 3p ionization. After accounting for these uncertainties, there appears to be no significant projectile mass or sign of charge effects for the ejected electron portion of the spectrum, which our CTMC results show is the dominant process for scaled velocities of less than approximately 0.5. However, our CTMC results show significant differences due to projectile charge, both in the ejected electron and the scattered projectile cross-sections, for collisions where the energy transfer is large. Currently, we are not aware of any positron data for directly testing these observations.

In Figure 2, the angular distributions for electron emission for 100, 250, and 500 eV electron impact (blue symbols) [20,21] are compared with 0.2, 0.5, and 1 MeV proton impact data [22]. Included in the comparison are normalized data for 120 eV positron impact (open and filled red symbols) [25]. The calculated ejected electron and scattered projectile cross-sections for 500 eV electron and positron impact are shown as blue and red solid and dashed curves. For clarity, the intermediate and highest energy data were divided by 10 and 100, respectively. In making these comparisons, it is again important to remember that the electron impact data are the sum of the scattered projectile and ejected electron signals, whereas the proton data is only the ejected electron portion. However, for positron impact and our CTMC results, the scattered projectile and ejected electron cross-sections are independently determined.
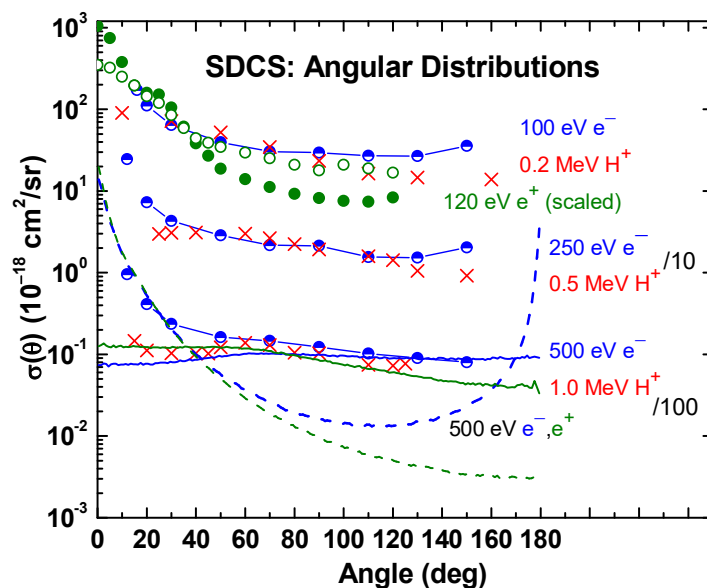
Figure 2. Single differential cross-section angular distributions for 100, 250, and 500 eV electron impacts (half-filled blue circles) [20,21]; 120 eV positron impact (open and filled green circles, scaled; see text) [25] (0.2 Crooks and Rudd, ref. [22]; 0.5 Gabler et al., ref. [22]; 1.0 MeV Toburen, ref. [22]) and proton impact (red symbols); and our CTMC results for 500 eV electron and positron impact (blue and green lines, respectively). The solid curves are the ejected electrons and the dashed curves the scattered projectile contributions. The intermediate and high energy data are divided by 10 and 100, respectively, for display purposes.

Using our CTMC results as a guide, we see that for electron impact the cross-sections in the forward and backward directions are dominated by the scattered projectile contribution. In the forward direction, our CTMC results indicate very little difference between positive and negative projectiles, whereas in the backward direction, projectile scattering is much more important for electron impact than for positron impact. This, as mentioned in the introduction, can be associated with the direction of scattering since the partially screened nuclear charge can more strongly interact with the outgoing projectile electron, which can lead to more scattering at large angles.

Turning our attention to the ejected electron distributions, both our CTMC calculations and the data of Falke et al. [25] show that ejection of a target electron is more probable than projectile scattering at intermediate angles. Lastly, comparing our CTMC results for ejected electrons, the angular distribution is fairly constant for electron impact, whereas it decreases with the angle for positron impact. Thus, in the forward/backward directions, the ejection of a target electron is more/less probable for a negatively charged projectile than for a positively charged projectile. This can also be associated with the direction of scattering, since for a binary collision, the target electron is propelled in the forward direction away from/toward the partially screened nucleus for electron/positron impact. Hence, subsequent forces by the screened nucleus should cause some of the forward emission to shift to larger angles for positron impact.

3.3. Double Differential Cross-Sections (DDCS)

The next step in increasing the sensitivity is to compare data where both the energy and angle of the post-collision particles are known. Typically, both experiment and theory have concentrated on determining these for the ejected target electrons. However, similar data can be measured for the scattered projectiles. For argon, electron and proton data are available [20–22], and for positron impact, a very limited amount of data are available [26–29]. These, along with our CTMC results for both electron and positron impact, are compared and are shown in Figure 3. We note that in comparing these experimental data with our

one-electron model, on the DDCS level, single ionization is known to dominate for electron impact [30]. Based on this, we assume that the same applies for positron and proton impact.
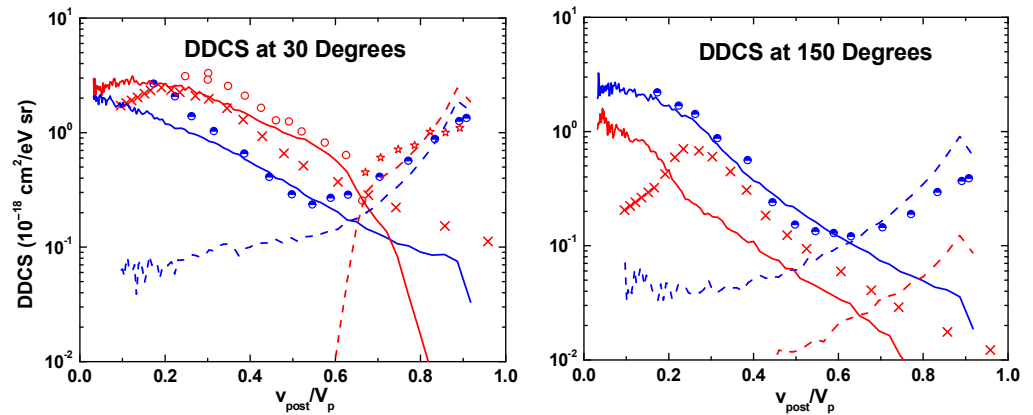

Figure 3. Double differential cross-sections for 100 eV electrons (half-filled blue circles) [20,21] and positrons (open red circles and stars) [27]; 0.2 MeV protons (red x) (Crooks and Rudd, ref. [22]); and our CTMC results for electron and positron impact (blue and red lines, respectively). The solid curves are for the ejected electrons and the dashed curves for the scattered projectile contributions.

Uncertainties in the electron and proton data are ~±25%. Uncertainties for the positron data, due to normalization and limited statistics are larger. Larger uncertainties are also expected for the experimental data at the smallest emission energies, i.e., for scaled velocities of less the 0.2. With this in mind, the data and CTMC results both show that electron emission caused by positive particle impact is larger than that caused by negative particle impact. For projectile scattering, both the data and CTMC results show a larger cross-section for positron impact in the forward direction. But, in the backward direction, the positron scattering cross-sections are an order of magnitude smaller than for electron impact, in accordance with one of the expectations mentioned in the introduction.

Regarding these features for projectile scattering, we note that the relative DDCS measurements of projectile energy loss at zero degrees for positron impact [26] showed nearly identical decreases with increasing energy loss, which is in agreement with our CTMC SDCS results, see Figure 1. But, because the positron and electron impact data were normalized to each other, no information about which cross-section is largest is available. However, the similar cross-sections for electron and positron scattering in the forward directions after target ionization are extremely similar to what is seen in elastic scattering, as shown in Figure 4, where experiment [31] and theory [32] are in good agreement. We note that the optical model used includes absorption processes, which may account for the similar features to the DDCS.

In Figure 5, DDCS for 15 eV electron emission from argon by electrons, protons, and positrons are shown. Note that the experimental data from Schmitt et al. [29] were originally placed on an absolute scale via a best fit to calculations for molecular hydrogen. In making the present comparison, we found poor agreement, both in magnitude and shape, with the other data in Figure 5. Therefore, here the magnitude of the Schmitt et al. data was increased by seven for electron impact data and by two for positron data; plus, both were divided by sin(θ). A possible explanation for the sin(θ) correction is that the experiment used a target emerging from a multicappilary orifice. Thus, depending on the beam target overlap, the target density could be modeled as a uniform jet or a static gas, the latter of which requires a sin(θ) correction. The figure shows that with the sin(θ) correction, good agreement with the positron data of Kövér et al. [27] and the electron data of DuBois [20,21] is achieved. The angular dependence in Figure 5 supports what was found above, namely larger cross-sections in the forward direction when the projectile charge is positive and in the backward direction when the projectile charge is negative.
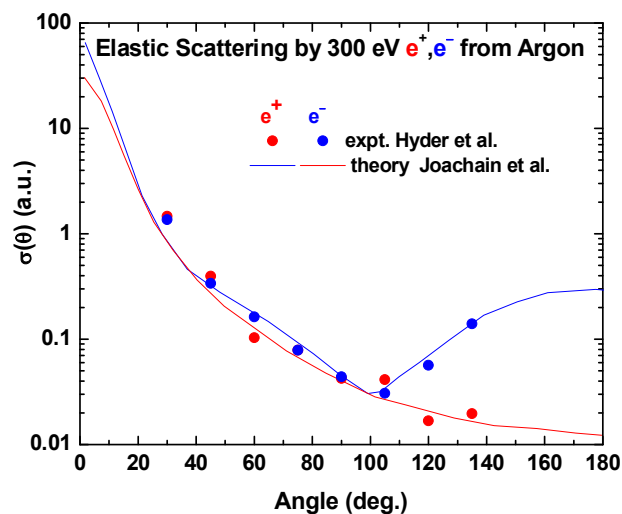
Figure 4. Elastic scattering from argon by 300 eV electrons and positrons. Experimental data from Hyder et al. [31]; theory by Joachain et al. [32].
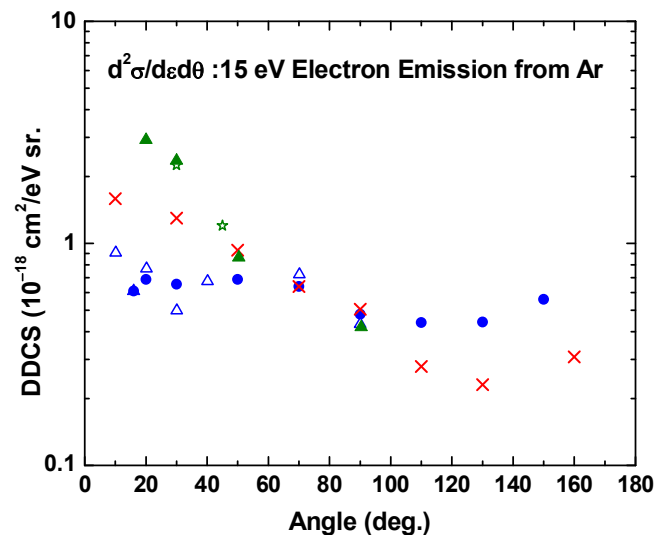

Figure 5. Double differential cross-sections for 15 eV electron emission from argon resulting from 100 eV electron (blue-filled circles [20] and open triangles [29]), positron (green-filled triangles [29] and open stars [27]), and 200 keV proton [22] impact (red cross). The positron data of Schmitt et al. [29] were adjusted in magnitude and shape. See text for details.

4. Summary and Possible Future Investigations

Experimentally obtained single and double differential data resulting from particle (electron and proton) and antiparticle (positron) impact ionization of argon were compared. Comparisons with CTMC calculations, where the ionized electron and scattered projectile contributions were independently computed, were also performed. The purpose of this study was to investigate whether projectile mass or the sign of charge effects are evident in data which, when compared to fully differential data, are much more able to experimentally feasible for antiparticle impact. Our findings from the comparisons can be briefly summarized as follows.

TCS: For impact velocities greater than 2 a.u., any differences in the total cross-sections due to a projectile mass or sign of charge are a few percent level or smaller. Differences were noted for smaller velocities, but in this region, any comparisons require data where contributions from the various contributing channels are known.

SDCS-energy distributions: From a comparison of single differential energy distributions for electron and proton impact, no differences were observed for energies where

ejected electrons dominate, i.e., velocities of less than half the beam velocity. Only a single measurement for positron impact is currently available; more positron measurements would be useful. We note that, in this region, the cross-sections are much smaller than the total cross-sections. An interesting area for future investigations is the large energy transfer where our CTMC results imply large differences between electron and positron impact, particularly for the scattered projectile channel. But the cross-sections in this region are quite small, meaning experimental investigations will be difficult.

SDCS-angular distributions: The main difference in the angular dependences for electron and proton impact is in the very forward and backward directions. In these areas, differences are attributed to the importance of scattered projectiles. Only a single positron measurement is available at present. More positron data are needed where both the ejected electron and scattered projectile signals are independently measured. We note that, except for large angle scattering, where differences in electron impacts can be orders of magnitude, these cross-sections are only a factor of 5 to 10 smaller than the total cross-sections.

DDCS: Although antiparticle data are quite limited, the major finding is that for forward electron emission, the cross-sections for positively charged projectiles is larger than for negatively charged projectiles, whereas in the backward direction, it is just the opposite. More double differential antiparticle data are needed but, we note that the DDCS are more than 20 times smaller than SDCS.

According to the above summary we propose the possible future investigations as follows.

The primary need is additional single and double differential measurements for positron impact and, hopefully at some point, also for antiproton impact. From the comparisons presented here, angular dependences with emphasis on obtaining information at backward angles would be the most useful. Such data could be collected using a simple experimental setup, such as those used by Falke et al. [25] many years ago. Equally important are measurements where both the ejected electron and scattered projectile signals are measured on an absolute scale, perhaps by normalizing to elastic scattering data, which could also be measured using the same setup.

Various categorizations of our CTMC calculations also indicated other interesting avenues to pursue. One is obtaining some information about the impact parameters, and whether a method can be found that is appropriate for lepton impact. Another is that, according to our CTMC results, although positrons mainly are scattered "away" from the target and electrons are mainly scattered "toward" the target, i.e., larger/smaller radial distances from the incoming trajectory, a portion of the beam is scattered in the opposite direction. The preliminary calculations we performed indicate that the "opposite" scattering accounts for about 10% of the ionization at 1 keV with its importance being considerably more important at lower impact energies. The significance of this is that in binary collisions, the target electron is ejected in the opposite direction from the direction of projectile scattering. Thus, an electron ejected "toward" the target core is subject to a stronger field than one ejected "away" from the target core. Hence, any post-collision kinematic effects will be different for these two cases. Experimentally measuring the scattering direction might be possible using the sensitive measurements of the recoil ion. Whether this effect that we observed using our classical calculation can be incorporated into quantal calculations is a question worth pursuing.

In conclusion, we hope that the comparisons shown and the suggestions we have provided lead to new experimental studies and additional differential data for positron, and, someday, for antiproton impact.

Author Contributions: R.D.D. was responsible for the conceptualization and methodology of this work, as well as producing the original draft. K.T. was responsible for all aspects of the CTMC calculations. All authors have read and agreed to the published version of the manuscript.

Data Availability Statement: The data that support the findings of this study are available from the authors upon reasonable request.

Conflicts of Interest: The authors declare no conflict of interest.

References

1. DuBois, R.D. Methods and progress in studying inelastic interactions between positrons and atoms. *J. Phys. B At. Mol. Opt. Phys.* **2016**, *49*, 112002. [CrossRef]
2. Andersen, L.H.; Hvelplund, P.; Knudsen, H.; Møller, S.P.; Sørensen, A.H.; Elsener, K.; Rensfelt, H.-G.; Uggerhøj, E. Multiple ionization of He, Ne, and Ar by fast protons and antiprotons. *Phys. Rev. A.* **1987**, *36*, 3612. [CrossRef] [PubMed]
3. Paludan, K.; Bluhme, H.; Knudsen, H.; Mikkelsen, U.; Møller, S.P.; Uggerhøj, E.; Morenzoni, E. Single, double and triple ionization of Ne, Ar, Kr and Xe by 30–1000 keV p−Impact. *J. Phys. B At. Mol. Opt. Phys.* **1997**, *30*, 3951–3968. [CrossRef]
4. Knudsen, H.; Kristiansen, H.-P.E.; Thomsen, H.D.; Uggerhøj, U.I.; Ichioka, T.; Møller, S.P.; Hunniford, C.A.; McCullough, R.W.; Charlton, M.; Kuroda, N.; et al. Ionization of helium and argon by very slow antiproton impact. *Phys. Rev. Lett.* **2008**, *101*, 043201-1–043201-4. [CrossRef] [PubMed]
5. Knudsen, H.; Torii, H.A.; Charlton, M.; Enomoto, Y.; Georgescu, I.; Hunniford, C.A.; Kim, C.H.; Kanai, Y.; Kristiansen, H.-P.E.; Kuroda, N.; et al. Target Structure Induced Suppression of the Ionization Cross Section for Very Low Energy Antiproton-Hydrogen Collisions. *Phys. Rev. Lett.* **2010**, *105*, 213201. [CrossRef] [PubMed]
6. Arcidiacono, C.; Kövér, Á.; Laricchia, G. Energy-Sharing Asymmetries in Ionization by Positron Impact. *Phys. Rev. Lett.* **2005**, *95*, 223202. [CrossRef] [PubMed]
7. Ren, X.; Senftleben, A.; Pflüger, T.; Dorn, A.; Bartschat, K.; Ullrich, J. Low-energy Electron-impact Ionization of Argon: Three dimensional Cross Section. *Phys. Rev. A* **2012**, *85*, 032702. [CrossRef]
8. DuBois, R.D.; de Lucio, O.G. Triply Differential Positron and Electron Impact Ionization of Argon: Systematic Features and Scaling. *Atoms* **2021**, *9*, 78. [CrossRef]
9. Naja, A.; Staicu-Casagrande, E.M.; Lahmam-Bennani, A.; Nekkab, M.; Mezdari, F.; Joulakian, B.; Chuluunbaatar, O.; Madison, D.H. Triply differential (e,2e) cross sections for ionization of the nitrogen molecule at large energy transfer. *J. Phys. B At. Mol. Opt. Phys.* **2007**, *40*, 3775–3783. [CrossRef]
10. Purohit, G.; Kato, D. Projectile-charge dependence of the differential cross section for the ionization of argon atoms at 1 keV. *Phys. Rev. A* **2017**, *96*, 042710. [CrossRef]
11. Tőkési, K.; DuBois, R.D. Energy and angular distributions in 250 eV electron and positron collisions with argon atom. *J. Phys. B At. Mol. Opt. Phys.* **2023**. *to be published*.
12. Green, A.E.S. An Analytic Independent Particle Model for Atoms: I. Initial Studies. *Adv. Quantum Chem.* **1973**, *7*, 221–262.
13. Garvey, R.H.; Jackman, C.H.; Green, A.E.S. Independent-particle-model potentials for atoms and ions with 36 < Z ≤ 54 and a modified Thomas-Fermi atomic energy formula. *Phys. Rev. A* **1975**, *12*, 1144.
14. Reinhold, C.O.; Falcón, C.A. Classical ionization and charge-transfer cross sections for H+ + He and H+ + Li+ collisions with consideration of model interactions. *Phys. Rev. A* **1986**, *33*, 3859. [CrossRef] [PubMed]
15. McCallion, P.; Shah, M.B.; Gilbody, H.B. A crossed beam study of the multiple ionization of argon by electron impact. *J. Phys. B At. Mol. Opt. Phys.* **1992**, *25*, 1061. [CrossRef]
16. Bluhme, H.; Knudsen, H.; Merrison, J.P.; Nielsen, K.A. Ionization of argon and krypton by positron impact. *J. Phys. B At. Mol. Opt. Phys.* **1999**, *32*, 5835. [CrossRef]
17. Jacobsen, F.M.; Frandsen, N.P.; Knudsen, H.; Mikkelsen, U.; Schrader, D.M. Single ionization of He, Ne and Ar by positron Impact. *J. Phys. B At. Mol. Opt. Phys.* **1995**, *28*, 4691. [CrossRef]
18. DuBois, R.D.; Manson, S.T. Multiple-ionization channels in proton-atom collisions. *Phys. Rev. A* **1987**, *35*, 2007–2025. [CrossRef]
19. Montanari, D.; Miraglia, J.E. Positron and electron-impact multiple-ionization. *J. Phys. B At. Mol. Opt. Phys.* **2015**, *48*, 165203. [CrossRef]
20. DuBois, R.D. Absolute Differential Cross Sections for 20–800 eV e− Ar and e− N_2 Collisions for Elastic Scattering and Secondary Electron Production. Ph. D. Thesis, University of Nebraska, Lincoln, NE, USA, 1975.
21. DuBois, R.D.; Rudd, M.E. Absolute Doubly Differential Cross Sections for Ejection of Secondary Electrons from Gases by Electron Impact II: 100–500 eV Electron Impact on Neon, Argon, Molecular Hydrogen and Molecular Nitrogen. *Phys. Rev. A* **1978**, *17*, 843–848. [CrossRef]
22. Rudd, M.E.; Toburen, L.H.; Stolterfoht, N. Differential Cross Sections for Ejection of electrons from Argon by Protons. *At. Data Nucl. Data Tables* **1979**, *23*, 405–442. [CrossRef]
23. Moxom, J.; Laricchia, G.; Charlton, M. Jones and Kövér, Á. Ionization of He, Ar and Hz by positron impact at intermediate energies. *J. Phys. B At. Mol. Opt. Phys.* **1992**, *25*, L613. [CrossRef]
24. Rudd, M.E. Differential cross sections for secondary electron production by proton impact. *Phys. Rev. A* **1988**, *38*, 6129. [CrossRef] [PubMed]
25. Falke, T.; Brandt, T.; Kühl, O.; Raith, W.; Weber, M. Differential Ps-formation and impact-ionization cross sections for positron scattering on Ar and Kr atoms. *J. Phys. B At. Mol. Opt. Phys.* **1997**, *30*, 3247–3256. [CrossRef]

26. Kövér, Á.; Laricchia, G.; Charlton, M. Ionization by positrons and electrons of Ar at zero degrees. *J. Phys. B At. Mol. Opt. Phys.* **1993**, *26*, L575. [CrossRef]

27. Kövér, Á.; Laricchia, G.; Charlton, M. Doubly differential cross sections for collisions of 100 eV positrons and electrons with argon atoms. *J. Phys. B At. Mol. Opt. Phys.* **1994**, *27*, 2409. [CrossRef]

28. Kövér, Á.; Finch, R.M.; Charlton, M.; Laricchia, G. Doubly differential cross sections for collisions of 100 eV positrons with argon atoms. *J. Phys. B At. Mol. Opt. Phys.* **1997**, *30*, L507. [CrossRef]

29. Schmitt, A.; Cerny, U.; Möller, H.; Raith, W.; Weber, M. Positron-atom doubly differential ionization cross sections. *Phys. Rev. A* **1994**, *49*, R5. [CrossRef]

30. Chaudhry, M.A.; Duncan, A.J.; Hippler, R.; Kleinpoppen, H. Partial doubly differential cross sections for multiple ionization of argon, krypton, and xenon atoms by electron impact. *Phys. Rev A* **1989**, *39*, 530–539. [CrossRef]

31. Hyder, G.M.A.M.; Dababneh, S.; Hsieh, Y.-F.; Kauppila, W.E.C.; Kwan, K.; Mahdavi-Hezaveh, M.; Stein, T.S. Positron Differential Elastic-Scattering Cross-Section Measurements for Argon. *Phys. Rev. Lett.* **1986**, *57*, 2252. [CrossRef]

32. Joachain, C.J.; Vanderpoorten, R.; Winters, K.-H.; Byron, F.J. Optical model theory of elastic electron- and positron-argon scattering at intermediate energies. *J. Phys. B At. Mol. Opt. Phys.* **1977**, *10*, 227. [CrossRef]